TRANSIENT EFFECTS IN ELASTODYNAMIC FRACTURE OF GRADED MATERIALS

A. Shukla and N. Jain
Dynamic Photomechanics Laboratory.
Department of Mechanical Engineering and Applied Mechanics, University of Rhode Island
110 Wales Hall, 92 Upper College Rd., Kingston, RI 02881-0805, USA

ABSTRACT

The transient nature of elastodynamic crack growth in graded materials under plane stress and plane strain is considered. Crack tip stress, strain and displacement fields for a transient crack propagating along the direction of property gradation in functionally graded materials (FGMs) are obtained through an asymptotic analysis coupled with displacement potential approach. The influence of transient nature of crack tip on contours of constant maximum shear stress is discussed.

1. INTRODUCTION

The elastic stress, strain and displacement fields for a crack propagating at a nonuniform speed along the direction of property variation in an FGM are developed. The elastodynamic problem is formulated in terms of displacement potentials through an asymptotic analysis for opening mode. The properties are assumed to vary exponentially along the direction of crack propagation. In this context, transient crack growth is understood to include processes in which both the crack tip speed and dynamic stress intensity factor are differentiable functions of time.

A functionally graded material (FGM) is a composite consisting, of two or more phases, which is fabricated such that its composition varies in a defined spatial direction. The design is intended to take advantage of certain desirable features of each of the constituent phases. Extensive efforts have been made to characterize the crack tip stress field in FGMs under quasi-static loading. Erdogan [1] has shown that for a general nonhomogeneous material the quasi-static crack-tip stress field exhibits classical inverse square root singularity if the spatial variation of elastic properties is continuous. In contrast with the relatively extensive literature on the quasi-static behavior of cracks in FGMs, only a few investigations study the dynamic fracture of FGMs [2,3]. In most of the studies previously performed on propagating cracks in FGMs, the crack tip speed was assumed to be constant. The transient solution for elastodynamic crack growth in FGMs provides a strong foundation for the interpretation of experimental measurement in dynamic fracture testing of these materials. The transient stress fields developed in this paper are used to generate the contours of constant maximum shear stress (isochromatics) and the effect of transient crack growth on these contours is discussed.

2. THEORETICAL FORMULATION

Consider an FGM with exponentially varying elastic modulus and constant density, occupying the *X-Y* two-dimensional space. Let us assume that the FGM contains a crack with faces parallel to the *X-Z* plane, propagating at a non-uniform velocity *c(t)* in the positive *X* direction.

The elastic constants μ and λ and the density ρ are assumed to vary in an exponential manner given by Eq. (1), whereas the Poisson's ratio ν is assumed to be constant.

$$\mu = \mu_0 \exp(\alpha X),\ \rho = \rho_0 \exp(\alpha X). \tag{1}$$

μ_0 and ρ_0 are the shear modulus and mass density at X=0 and α is a constant having dimension (Length)$^{-1}$.

Within the framework of plane elasticity the equations of motion for any elastodynamic problem can be written as

$$\frac{\partial \sigma_{XX}}{\partial X}+\frac{\partial \sigma_{XY}}{\partial Y}=\rho\frac{\partial^2 u}{\partial t^2},$$
$$\frac{\partial \sigma_{XY}}{\partial X}+\frac{\partial \sigma_{YY}}{\partial Y}=\rho\frac{\partial^2 v}{\partial t^2}. \tag{2}$$

where σ_{ij} are the in-plane stress components and u, v are in-plane displacements.

Stress can be expressed in terms of displacements using Hooke's law as

$$\sigma_{XX}=\left(\left(\lambda_0+2\mu_0\right)\frac{\partial u}{\partial X}+\lambda_0\frac{\partial v}{\partial Y}\right)\exp(\alpha X),$$
$$\sigma_{YY}=\left(\left(\lambda_0+2\mu_0\right)\frac{\partial v}{\partial Y}+\lambda_0\frac{\partial u}{\partial X}\right)\exp(\alpha X), \tag{3}$$
$$\sigma_{XY}=\left(\frac{\partial u}{\partial Y}+\frac{\partial v}{\partial X}\right)\mu_0\exp(\alpha X).$$

where λ_0 is Lame's constant at crack tip.

In plane displacements, u and v, can be expressed in terms of displacement potentials (Φ and Ψ) as

$$u=\frac{\partial \Phi}{\partial X}+\frac{\partial \Psi}{\partial Y},$$
$$v=\frac{\partial \Phi}{\partial Y}-\frac{\partial \Psi}{\partial X}. \tag{4}$$

Substituting Eq. (4) into Eq. (3) and substituting the resulting equation into Eq. (2), the equation of motion can be expressed in terms of displacement potentials Φ and Ψ as

$$\frac{\partial}{\partial X}\left\{(k+2)\nabla^2\Phi-\frac{\rho_0}{\mu_0}\frac{\partial^2\Phi}{\partial t^2}\right\}+\frac{\partial}{\partial Y}\left\{\nabla^2\Psi-\frac{\rho_0}{\mu_0}\frac{\partial^2\Psi}{\partial t^2}\right\}+\alpha\left\{k\nabla^2\Phi+2\frac{\partial^2\Phi}{\partial X^2}+2\frac{\partial^2\Psi}{\partial X\partial Y}\right\}=0,$$
$$\frac{\partial}{\partial Y}\left\{(k+2)\nabla^2\Phi-\frac{\rho_0}{\mu_0}\frac{\partial^2\Phi}{\partial t^2}\right\}-\frac{\partial}{\partial X}\left\{\nabla^2\Psi-\frac{\rho_0}{\mu_0}\frac{\partial^2\Psi}{\partial t^2}\right\}+\alpha\left\{\frac{\partial^2\Psi}{\partial Y^2}-\frac{\partial^2\Psi}{\partial X^2}+2\frac{\partial^2\Phi}{\partial X\partial Y}\right\}=0. \tag{5}$$

where $k=\lambda_0/\mu_0$

After some mathematical manipulations it can be shown that Eq. (5) can be only satisfied when addressed as

$$(k+2)\nabla^2\Phi-\frac{\rho_0}{\mu_0}\frac{\partial^2\Phi}{\partial t^2}+\alpha\frac{\partial\Psi}{\partial Y}+\alpha(k+2)\frac{\partial\Phi}{\partial X}=0,$$
$$\nabla^2\Psi-\frac{\rho_0}{\mu_0}\frac{\partial^2\Psi}{\partial t^2}+\alpha k\frac{\partial\Phi}{\partial Y}+\alpha\frac{\partial\Psi}{\partial X}=0. \tag{6}$$

For transient crack tip analysis, Eq. (6) can be written in the crack-tip moving coordinate reference (x, y) using the transformations given below.

$$x = X-ct,\ y = Y$$
$$\frac{\partial^2}{\partial X^2}=\frac{\partial^2}{\partial x^2};\qquad \frac{\partial^2}{\partial t^2}=c^2\frac{\partial^2}{\partial x^2}+\frac{\partial^2}{\partial t^2}-\dot{c}\frac{\partial}{\partial x}-2c\frac{\partial^2}{\partial x\partial t} \tag{7}$$
$$\text{where } \dot{c}=\frac{\partial c}{\partial t}$$

Using the transformed crack-tip coordinates, Eq. (7) can be rewritten as

$$\alpha_l^2\frac{\partial^2\Phi}{\partial x^2}+\frac{\partial^2\Phi}{\partial y^2}+\alpha\frac{\partial\Phi}{\partial x}-\frac{\alpha}{k+2}\frac{\partial\Psi}{\partial y}+\frac{\rho_0}{\mu_0(k+2)}\left\{\dot{c}\frac{\partial\Phi}{\partial x}+2c\frac{\partial^2\Phi}{\partial x\partial t}-\frac{\partial^2\Phi}{\partial t^2}\right\}=0,$$
$$\alpha_s^2\frac{\partial^2\Psi}{\partial x^2}+\frac{\partial^2\Psi}{\partial y^2}+\alpha\frac{\partial\Psi}{\partial x}+\alpha k\frac{\partial\Phi}{\partial y}\frac{\rho_0}{\mu_0(k+2)}\left\{\dot{c}\frac{\partial\Psi}{\partial x}+2c\frac{\partial^2\Psi}{\partial x\partial t}-\frac{\partial^2\Psi}{\partial t^2}\right\}=0. \tag{8}$$

where, $\alpha_l=\left(1-\frac{\rho_0c^2}{\mu_0(k+2)}\right)^{1/2}$, $\alpha_s=\left(1-\frac{\rho_0c^2}{\mu_0}\right)^{1/2}$.

It should be noticed here that by setting the nonhomogeneity parameter (α) equal to zero these equations reduce to the corresponding equations of motion for homogeneous materials. However, due to the nonhomogeneous nature of the material, these equations (8) lose their classical form and remain coupled in the two fields Φ and Ψ, through the nonhomogeneity parameter α.

To derive an asymptotic expansion for the stress components near the crack tip a standard method is employed in which the region around the crack tip is expanded so to fill the entire field of observation**.** To this end, rescaled coordinates $\eta_1=x/\varepsilon$, $\eta_2=y/\varepsilon$, $0<\varepsilon<1$ are introduced. As $\varepsilon\to 0$, all points in the x-y plane except those near the crack tip are mapped beyond range of observation in the η_1, η_2 plane.

Assuming Φ and Ψ can be expressed in powers of ε as

$$\Phi(x,y)=\Phi(\varepsilon\eta_1,\varepsilon\eta_2)=\sum_{m=0}^{\infty}\varepsilon^{\frac{m+3}{2}}\phi_m(\eta_1,\eta_2),$$
$$\Psi(x,y)=\Psi(\varepsilon\eta_1,\varepsilon\eta_2)=\sum_{m=0}^{\infty}\varepsilon^{\frac{m+3}{2}}\psi_m(\eta_1,\eta_2). \tag{9}$$

The first term of series (m=0) corresponds to the expected square root singular contribution proportional to $r^{-1/2}$ in the asymptotic near-tip stress field.

Substituting the assumed asymptotic form (9) in to governing equation (8) and using the scaled coordinates an infinite series involving differential equations associated with each power of ε is obtained**.** For the resulting equation to be valid the differential equations corresponding to each power of ε ($\varepsilon^{3/2}$, ε^2, $\varepsilon^{5/2}$...) should vanish independently. By setting each power of ε equal to zero will lead to a set of coupled partial differential equations in ϕ and ψ. In particular for any value of m, these governing equations will have a general from as

$$\alpha_l^2\frac{\partial^2\phi_m}{\partial\eta_1{}^2}+\frac{\partial^2\phi_m}{\partial\eta_2{}^2}+\alpha\frac{\partial\phi_{m-2}}{\partial\eta_1}+\frac{\alpha}{k+2}\frac{\partial\psi_{m-2}}{\partial\eta_2}+\frac{\rho_0c^{1/2}}{\mu_0(k+2)}\frac{\partial}{\partial t}\left\{c^{1/2}\frac{\partial\phi_{m-2}}{\partial\eta_1}\right\}-\frac{\rho_0}{\mu_0(k+2)}\frac{\partial^2\phi_{m-4}}{\partial t^2}=0$$
$$\alpha_s^2\frac{\partial^2\psi_m}{\partial\eta_1{}^2}+\frac{\partial^2\psi_m}{\partial\eta_2{}^2}+\alpha\frac{\partial\psi_{m-2}}{\partial\eta_1}+\alpha k\frac{\partial\phi_{m-2}}{\partial\eta_2}+\frac{\rho_0c^{1/2}}{\mu_0}\frac{\partial}{\partial t}\left\{c^{1/2}\frac{\partial\psi_{m-2}}{\partial\eta_1}\right\}-\frac{\rho_0}{\mu_0(k+2)}\frac{\partial^2\psi_{m-4}}{\partial t^2}=0 \tag{10}$$

where

$$\phi_k,\psi_k=\begin{cases}\phi_k,\psi_k & for\ \ k\geq 0\\ 0 & for\ \ k<0\end{cases}$$

For m = 0 and 1 (Eq. (10)) remains uncoupled and exactly similar to that for a homogeneous material having elastic properties same as that of the elastic properties of the FGM at the crack tip. Indeed, as will be seen, ϕ_0 and ψ_0 have the same spatial structure in both transient and steady state cases. This is not so, however, for ϕ_m, ψ_m if $m > 1$.

The governing equations (10) for m = 0 and 1 can be easily reduced to Laplace's equations in the respective complex domains $\varsigma_l=\eta_1+i\alpha_l\eta_2$, $\varsigma_s=\eta_1+i\alpha_s\eta_2$, $i=\sqrt{-1}$.

For opening mode, the crack face boundary conditions can be given as

$$\sigma_{YY} = \sigma_{XY} = 0 \ for\ (x<0, Y=0)\ and\ \sigma_{XY} = 0\ for (Y=0) \tag{11}$$

Using theses boundary conditions the solution to the partial differential equation (10) corresponding to $m = 0$ and 1, can be given as

$$\begin{aligned} \phi_m(\rho_l,\theta_l,t) &= A_m(t) r_l^{(m+3)/2} \cos\frac{1}{2}(m+3)\theta_l, \\ \psi_m(\rho_s,\theta_s,t) &= B_m(t) r_s^{(m+3)/2} \sin\frac{1}{2}(m+3)\theta_s. \end{aligned} \qquad m = 0,\ 1 \tag{12}$$

where

$$\rho_l = \left[\eta_1^2 + \alpha_l^2\eta_2^2\right]^{1/2},\ \tan\theta_l = \frac{\alpha_l\eta_2}{\eta_1},\ \ \rho_s = \left[\eta_1^2 + \alpha_s^2\eta_2^2\right]^{1/2} \text{ and } \tan\theta_s = \frac{\alpha_s\eta_2}{\eta_1}$$

It should be emphasized here that (ρ_l,θ_l) and (ρ_s,θ_s) are translating polar coordinates distorted from conventional polar coordinates by an amount determined by the crack speed c. As crack speed is now a function of time, coordinates (ρ_l,θ_l) and (ρ_s,θ_s) are now dependent on time. Using the definition of the time dependent dynamic stress intensity factor, $K_{ID}(t) = \underset{\substack{r\to 0\\ \theta\to 0}}{Lim}\ \ \sigma_{yy}\sqrt{2\pi r}$, and the crack face boundary condition, $\sigma_{xy} = 0$ on $Y = 0$, the coefficients A_0 and B_0 can be determined as

$$A_0(t) = \frac{4(1+\alpha_s^2)}{3(4\alpha_s\alpha_l - (1+\alpha_s^2)^2)}\frac{K_{ID}(t)}{\mu_c\sqrt{2\pi}},\ \ B_0(t) = -\frac{2\alpha_l}{1+\alpha_s^2}A_0(t). \tag{13}$$

For $m = 2$ governing equation (10) reduces to

$$\begin{aligned} &\alpha_l^2\frac{\partial^2\phi_2}{\partial\eta_1^2} + \frac{\partial^2\phi_2}{\partial\eta_2^2} + \alpha\frac{\partial\phi_0}{\partial\eta_1} + \frac{\alpha}{k+2}\frac{\partial\psi_0}{\partial\eta_2} + \frac{\rho_0 c^{1/2}}{\mu_0(k+2)}\frac{\partial}{\partial t}\left\{c^{1/2}\frac{\partial\phi_0}{\partial\eta_1}\right\} = 0, \\ &\alpha_s^2\frac{\partial^2\psi_2}{\partial\eta_1^2} + \frac{\partial^2\psi_2}{\partial\eta_2^2} + \alpha\frac{\partial\psi_0}{\partial\eta_1} + \alpha k\frac{\partial\phi_0}{\partial\eta_2} + \frac{\rho_0 c^{1/2}}{\mu_0}\frac{\partial}{\partial t}\left\{c^{1/2}\frac{\partial\psi_0}{\partial\eta_1}\right\} = 0. \end{aligned} \tag{14}$$

Solution to the governing equation (14) can be given as

$$\begin{aligned} \phi_2 &= A_2(t)\rho_l^{5/2}\cos\frac{5}{2}\theta_l - \frac{1}{4\alpha_l^2}\alpha A_0(t)\rho_l^{5/2}\cos\frac{1}{2}\theta_l - \frac{2}{5}\frac{\alpha\alpha_s}{(k+2)(\alpha_l^2-\alpha_s^2)}B_0(t)\rho_s^{5/2}\cos\frac{5}{2}\theta_s \\ &+ \rho_l^{5/2}\left\{\frac{1}{6}[D_l^1\{A_0(t)\} + \frac{1}{2}B_l(t)\cos\frac{\theta_l}{2}] - \frac{1}{8}B_l(t)\cos\frac{3\theta_l}{2}\right\} \\ \psi_2 &= B_2(t)\rho_s^{5/2}\sin\frac{5}{2}\theta_s - \frac{1}{4\alpha_s^2}\alpha B_0(t)\rho_s^{5/2}\sin\frac{1}{2}\theta_s - \frac{2}{5}\frac{\alpha\alpha_l}{(k+2)(\alpha_l^2-\alpha_s^2)}A_0(t)\rho_l^{5/2}\sin\frac{5}{2}\theta_l \\ &+ \rho_s^{5/2}\left\{\frac{1}{6}[D_s^1\{B_0(t)\} + \frac{1}{2}B_s(t)]\sin\frac{\theta_s}{2} + \frac{1}{8}B_s(t)\sin\frac{3\theta_s}{2}\right\} \end{aligned} \tag{15}$$

where $D_l^1\{A_0(t)\} = -\dfrac{3c^{1/2}\rho_0}{\alpha_l^2\mu_0(k+2)}\dfrac{d}{dt}\left\{c^{1/2}\dfrac{(1+\alpha_s^2)}{(4\alpha_s\alpha_l - (1+\alpha_s^2)^2)}K_{ID}(t)\right\}$

$$D_s^1\{B_0(t)\} = -\frac{3c^{1/2}\rho_0}{\alpha_s^2\mu_0}\frac{d}{dt}\left\{c^{1/2}\frac{2\alpha_l}{(4\alpha_s\alpha_l - (1+\alpha_s^2)^2)}K_{ID}(t)\right\}$$

$$B_l(t) = \frac{3c^2}{2\alpha_l^4}\left(\frac{\rho_0}{\mu_0(k+2)}\right)^2 A_0(t)\frac{dc}{dt},\ \ B_s(t) = \frac{3c^2}{2\alpha_l^4}\left(\frac{\rho_0}{\mu_0}\right)^2 B_0(t)\frac{dc}{dt}.$$

2.1 Stress, Strain and Displacement Fields

The stress, strain displacement fields around the crack tip can now be obtained using displacement potentials (Φ and Ψ) found in the previous sections.
The in-plane displacements (*u, v*) can be obtained by substituting (Φ and Ψ) in Eq. (4). Once in – plane displacements are obtained; In-plane strains can be obtained using Eq. (16)

$$\varepsilon_{xx} = \frac{\partial u}{\partial x}, \qquad \varepsilon_{yy} = \frac{\partial v}{\partial y}, \qquad \varepsilon_{xy} = \frac{1}{2}\left(\frac{\partial u}{\partial y} + \frac{\partial v}{\partial x}\right). \tag{16}$$

By substituting Eq. (3) in to Eq. (2), in-plane stress component can be written in terms of displacement potentials Φ and Ψ as,

$$\begin{aligned}
\frac{\sigma_{xx}}{\mu_c} &= \left[\left(\frac{p+1}{p-1}\right)\frac{\partial^2\Phi}{\partial^2 X} + \left(\frac{3-p}{p-1}\right)\frac{\partial^2\Phi}{\partial^2 Y} + 2\frac{\partial^2\Psi}{\partial X\partial Y}\right]\exp(\alpha x) \\
\frac{\sigma_{yy}}{\mu_c} &= \left[\left(\frac{3-p}{p-1}\right)\frac{\partial^2\Phi}{\partial^2 X} + \left(\frac{p+1}{p-1}\right)\frac{\partial^2\Phi}{\partial^2 Y} - 2\frac{\partial^2\Psi}{\partial X\partial Y}\right]\exp(\alpha x) \\
\frac{\sigma_{xy}}{\mu_c} &= \left[-\frac{\partial^2\Psi}{\partial^2 X} + \frac{\partial^2\Psi}{\partial^2 Y} + 2\frac{\partial^2\Phi}{\partial X\partial Y}\right]\exp(\alpha x)
\end{aligned} \tag{17}$$

where $p = 3 - 4\nu$ for plane strain and $p = \dfrac{3-\nu}{1+\nu}$ for plane stress.
Individual expressions for stress, strain and displacements are not provided here due to limitation of space.

3. DISCUSSION OF SOLUTIONS

To get an insight into the effects of transient terms on dynamic fracture process, contours of constant maximum shear stress (isochromatics) are generated for opening mode loading conditions. The contours are generated for an assumed value of the dynamic stress intensity factor (coefficient A_0), whereas the higher order coefficients A_1, A_2, B_1 and B_2 are assumed to be zero. However the nonhomogeneity and transient specific parts of the higher order term $r^{1/2}$, which has A_0 and B_0 as the coefficients, is retained. The typical values of material properties and material thickness used in generating contours are as follows: Poisson's ratio = 0.3, shear modulus at the crack tip μ_c = 1 GPa, density at the crack tip ρ_c = 2000 kg/m^3, thickness t = 0.01m, nonhomogeneity parameter α = 0.50 m^{-1}.
Figure 1 shows the effect of rate of change of mode-I stress intensity factor ($dK_{ID}(t)/dt$) on contours of constant maximum shear stress for opening mode loading around the crack-tip corresponding to K_{ID} = 1.0 MPa-m$^{1/2}$, c = 650 ms^{-1}. The crack is assumed to be moving with a uniform velocity i.e. dc/dt = 0. The value of $dK_{ID}(t)/dt$ was varied over six orders of magnitude for generating the contours. The crack occupies negative x-axis and the crack tip is located at (0, 0). It can be observed from the figure that as the $dK_{ID}(t)/dt$ increases, the size and number of the fringes around the crack tip increases. As can be seen in figure 1(a) for $dK_{ID}(t)/dt$ = 0 the fringes have negligible tilt. High velocity has the tendency to cause a backward tilt in fringes but this is compensated by the gradient in Young's modulus, which is increasing in the direction of crack propagation. As the rate of change of dynamic stress intensity factor increases the fringes start tilting backward (Figure 1(b and c)). The significant changes in pattern of these contours around the crack-tip suggest that the transient terms can have a major influence on the crack-tip field.

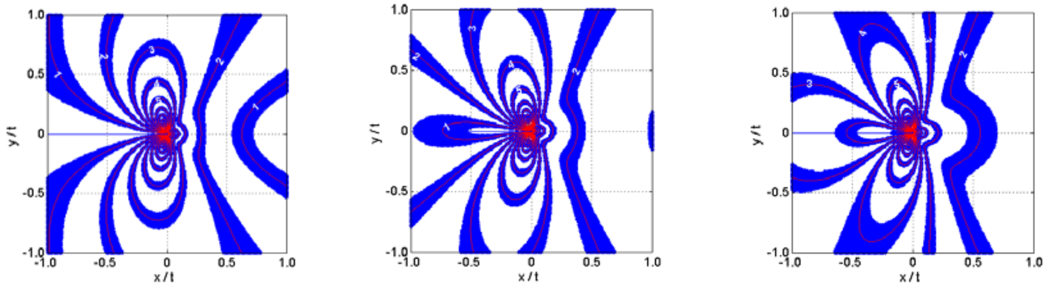

(a) $dK_{ID}/dt = 0$ (b) dK_{ID}/dt =1e5 MPa-m$^{1/2}$ s^{-1} (c) dK_{ID}/dt =1e6 MPa-m$^{1/2}$s^{-1}

Figure 1: Effect of rate of change of mode-I stress intensity factor on contours of constant maximum shear stress around the crack-tip

Figure 2 shows the effect of crack tip acceleration (*dc/dt*) on the contours of constant maximum shear stress. The value of *dc/dt* was varied over eight orders of magnitude. Changes in fringe size and shape up to crack tip accelerations of 10^6 ms^{-2} are negligible (figure 2a). Further increase in acceleration results in decrease in size of fringes around the crack tip (figures 2 b and c). It can also be observed that the fringes begin to tilt forward as the crack tip acceleration increases.

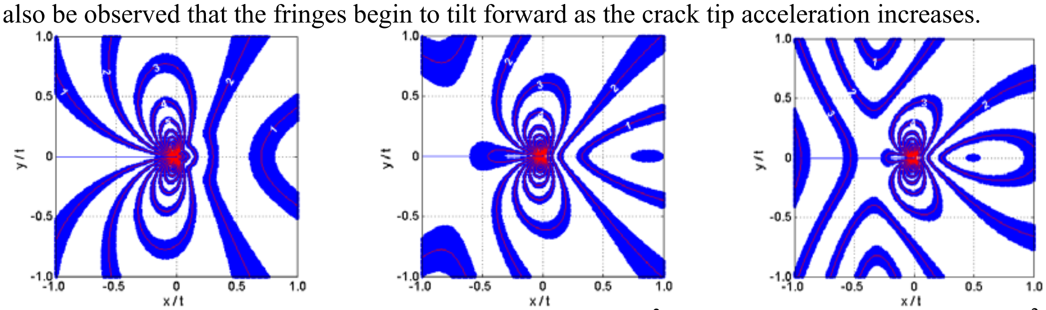

(a) *dc/dt* = 1 e 6 ms^{-2} (b) *dc/dt* = 1 e 7 ms^{-2} (c) *dc/dt* = 1 e 8 ms^{-2}

Figure 2: Effect of crack-tip acceleration on contours of constant maximum shear stress around the crack-tip for opening mode loading in an FGM

4. CLOSURE

Crack tip stress, strain and displacement fields for a transient crack propagating along the direction of property gradation were obtained through an asymptotic analysis coupled with displacement potential formulation. These stress fields are used to generate the synthetic contours of constant maximum shear stress. It was shown that transient effects causes significant spatial variation in these contours. Therefore, in studying dynamic fracture of FGMs, it is appropriate to include the higher order transient terms in the crack tip fields for the situations of sudden variation of stress intensity factor or crack tip velocity.

5. ACKNOWLEDGEMENTS

The authors would like to acknowledge the support of the National Science Foundation (NSF) under grant # CMS 0244330 and Office of Naval Research (ONR) under grant # N000140410268.

6. REFERENCES

1. Erdogan, F. “Fracture Mechanics of Functionally Graded Materials”, Comp. Eng, 5:7, 753-770, (1995).
2. Wang X. D. and Meguid S. A., “On the dynamic crack propagation in an interface with spatially varying elastic properties”, Int. J. Fract. 69, 87–99,1994;.
3. Parameswaran V., Shukla A., “Crack-tip stress field for dynamic fracture in functionally graded materials” Mech. Mat., 31,579-596,1999.